Water Research 255 (2024) 121460

Contents lists available at ScienceDirect

Water Research

journal homepage: www.elsevier.com/locate/watres

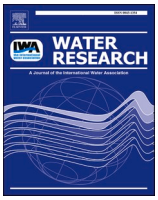

Reproducible responses of geochemical and microbial successional patterns in the subsurface to carbon source amendment

Jonathan P. Michael [a,b,1], Andrew D. Putt [c,1], Yunfeng Yang [d], Benjamin G. Adams [c], Kathryn R. McBride [e], Yupeng Fan [a,b], Kenneth A. Lowe [f], Daliang Ning [a,b], Sindhu Jagadamma [g], Ji Won Moon [h], Dawn M. Klingeman [f], Ping Zhang [i], Ying Fu [a,b], Terry C. Hazen [c,e,f,j,k], Jizhong Zhou [a,b,l,m,*]

[a] Institute for Environmental Genomics, University of Oklahoma, Norman, OK, USA
[b] School of Biological Sciences, University of Oklahoma, Norman, OK, USA
[c] Department of Earth and Planetary Sciences, University of Tennessee, Knoxville, TN, USA
[d] State Key Joint Laboratory of Environment Simulation and Pollution Control, School of Environment, Tsinghua University, Beijing, China
[e] Department of Microbiology, University of Tennessee, Knoxville, TN, USA
[f] Biosciences Division, Oak Ridge National Laboratory, Oak Ridge, TN, USA
[g] Biosystems Engineering and Soil Science, University of Tennessee, Knoxville, TN, USA
[h] National Minerals Information Center, United States Geological Survey, Reston, VA, USA
[i] Department of Molecular Virology and Microbiology, Baylor College of Medicine, Houston, TX, USA
[j] Department of Civil and Environmental Sciences, University of Tennessee, Knoxville, TN, USA
[k] Institute for a Secure and Sustainable Environment, University of Tennessee, Knoxville, TN, USA
[l] School of Civil Engineering and Environmental Sciences, University of Oklahoma, Norman, OK, USA
[m] Earth and Environmental Sciences, Lawrence Berkley National Laboratory, Berkeley, CA, USA

ARTICLE INFO

Keywords:
Community assembly
Groundwater contamination
Electron donor injection
Microbial succession

ABSTRACT

Carbon amendments designed to remediate environmental contamination lead to substantial perturbations when injected into the subsurface. For the remediation of uranium contamination, carbon amendments promote reducing conditions to allow microorganisms to reduce uranium to an insoluble, less mobile state. However, the reproducibility of these amendments and underlying microbial community assembly mechanisms have rarely been investigated in the field. In this study, two injections of emulsified vegetable oil were performed in 2009 and 2017 to immobilize uranium in the groundwater at Oak Ridge, TN, USA. Our objectives were to determine whether and how the injections resulted in similar abiotic and biotic responses and their underlying community assembly mechanisms. Both injections caused similar geochemical and microbial succession. Uranium, nitrate, and sulfate concentrations in the groundwater dropped following the injection, and specific microbial taxa responded at roughly the same time points in both injections, including *Geobacter, Desulfovibrio*, and members of the phylum Comamonadaceae, all of which are well established in uranium, nitrate, and sulfate reduction. Both injections induced a transition from relatively stochastic to more deterministic assembly of microbial taxonomic and phylogenetic community structures based on 16S rRNA gene analysis. We conclude that geochemical and microbial successions after biostimulation are reproducible, likely owing to the selection of similar phylogenetic groups in response to EVO injection.

1. Introduction

Electron donors, usually in the form of carbon compounds, are injected into the subsurface to enable biologically-mediated, *in situ* remediation of contaminants and have been widely adopted for large-scale projects because they are relatively inexpensive, environmentally

Abbreviations: EVO, emulsified vegetable oil; zOTU, zero-radius operational taxonomic unit.

* Corresponding author.
E-mail address: jzhou@ou.edu (J. Zhou).

[1] Co-first authors: Jonathan Michael and Andrew Putt

https://doi.org/10.1016/j.watres.2024.121460
Received 2 January 2024; Received in revised form 10 March 2024; Accepted 11 March 2024
Available online 13 March 2024
0043-1354/© 2024 The Authors. Published by Elsevier Ltd. This is an open access article under the CC BY-NC-ND license (http://creativecommons.org/licenses/by-nc-nd/4.0/).

friendly, and require less labor compared to physical or chemical methods (Borden and Rodriguez, 2006; Lakaniemi et al., 2019). In the case of uranium (U) contamination, carbon amendment stimulates microbially mediated reduction of U (Gandhi et al., 2022; Wall and Krumholz, 2006), which mitigates its mobility since oxidized hexavalent U (VI) is much more soluble in water than U (IV). U (VI) reduction is mediated by diverse phylogenetic and functional lineages, of which the most commonly reported are sulfate-reducing bacteria such as *Desulfovibrio* and iron-reducing bacteria such as *Geobacter*. In addition, other iron-reducing bacteria such as *Shewanella*, denitrifiers, cellulolytic bacteria, and spore-forming Firmicutes are commonly observed (Gihring et al., 2011; Ontiveros-Valencia et al., 2017; Wall and Krumholz, 2006).

Carbon amendments represent substantial perturbations to native microbial communities, and thus community succession following these amendments is a complex process that depends on numerous biotic and abiotic factors and their impacts and feedbacks on ecosystem processes. These interactions and feedbacks are controlled by both stochastic and deterministic community assembly mechanisms (Zhou and Ning, 2017). At our field site in Oak Ridge, TN, USA, waste from a legacy of uranium processing has left the groundwater contaminated with uranium, nitrate, sulfate, and numerous other contaminants. Conditions at the site fluctuate, but broadly, the microbiology at the site reflects the oligotrophic nature of groundwater, with community composition associated with levels of contamination, although there is also significant spatiotemporal variability (Fields et al., 2006; Lui et al., 2021; Smith et al., 2015; Thorgersen et al., 2015; Zelaya et al., 2019). However, the site has only occasionally been subjected to remedial actions and given the low quantities of carbon in the groundwater, any amendment would radically alter community structure and function (Chourey et al., 2013; Dangelmayr et al., 2019; Paradis et al., 2021). In one such amendment, emulsified vegetable oil (EVO) was injected into the groundwater in order to elucidate the impact of slow-release substrates on microbial community succession and associated biogeochemical processes. This injection, performed in 2009, caused U concentrations to drop from 1 to 3 mg mL^{-1} to <0.1 mg mL^{-1} for at least 4 weeks and promoted reducing conditions in the groundwater for at least 9 months (Gihring et al., 2011). A diverse consortium of organisms putatively responsible for individual steps of oil degradation was enriched. Key functional genes associated with EVO degradation and reduction of nitrate, sulfate, and uranium were sequentially altered during the course of the injection and correlated with geochemical conditions, which were indicative of selective enrichment of specific functional genes (Zhang et al., 2015). Null model analysis of the functional microarray data determined that the injection increased the importance of stochastic assembly on microbial functional groups (Zhou et al., 2014), while network analysis revealed increased network size as well as a shift towards competitive interactions following the injection (Deng et al., 2016). These findings contrast with network analysis of microbial communities in sediment following ethanol injection at the Oak Ridge site, which showed selection for overlapping or co-occurring biogeochemical processes (Li et al., 2018).

A different contaminated field site in Rifle, CO, USA, has also been subjected to carbon amendment. Acetate injection at this site resulted in microbially-mediated alteration of the physical structure of the subsurface. This likely resulted from pore-clogging as a consequence of organic carbon dynamics driven by selective processes, namely, the consumption of acetate by sulfate-reducing bacteria, which in turn affected the stochastic process of microbial dispersal (Dangelmayr et al., 2019; Li et al., 2010). At the same site, flow-through columns containing sediment were subjected to acetate amendment followed by lactate amendment at differing functional phases (iron- or sulfate-reducing) representing different initial community states. Investigators determined that community structure converged in response to lactate despite these differing initial states, revealing the deterministic impact of single-source injections (Handley et al., 2015). Thus, uncertainty exists as to the mechanisms by which microbial communities assemble if challenged with the same perturbation, and if subsequent injections would promote the same geochemical and microbial community impacts.

To further investigate, we compared the geochemical changes, microbial successional patterns, and community assembly processes of the Oak Ridge field site subjected to two EVO injections. Our objectives were to compare the biotic and abiotic impacts of both injections and their community assembly mechanisms. The first injection, conducted in 2009, used 680 L of EVO. The second injection was conducted in 2017, and used 208 L of EVO. We hypothesized that geochemical changes would be similar in both injections, with considerable reductions of nitrate, sulfate, and uranium (hypothesis i). If true, we expect that microbial community succession will also be similar (hypothesis ii). However, as a consequence of the increased importance of stochastic community assembly mechanisms based on functional gene community structures following EVO amendment (Zhou et al., 2014), we further hypothesized that microbial community composition between two injections would be highly dissimilar, particularly at the zOTU (zero-radius operational taxonomic unit, equivalent to an amplicon sequence variant), though changes in agglomerated indices, such as microbial abundance, α- and β-diversities, may be similar (hypothesis iii).

2. Materials and methods

2.1. Site description

Both injections took place in the Area 2 research site of the Y-12 national security complex in Oak Ridge, TN, USA, which has been described previously (Gihring et al., 2011). The three injection wells are approximately 300 m downstream of the S3 ponds, which are the contaminant center. Area 2 is less impacted by the S3 ponds than other areas at the Y-12 complex, but still contains roughly 2 mg L^{-1} uranium, up to 25 mg L^{-1} nitrate, and 50–70 mg L^{-1} sulfate. The pH in Area 2 is circumneutral, ranging from 6.4 to 7.6 during the monitoring period.

2.2. EVO injections

EVO injections in 2009 and 2017 utilized the same wells (FW212, FW213, FW214). Details of the 2009 injection have been described earlier (Gihring et al., 2011; Tang et al., 2013). The 2017 injection used a 20 % EVO solution generated by the thorough mixing of 832 L of pumped groundwater mixed with 208 L of 60 % SRS-SD EVO solution (Terra Systems Inc., Claymont, DE, USA) consisting of 60 % (wt/wt) soybean oil, 5.5 % food grade soluble substrate, <1 % proprietary food-grade nutrients, 7.5 % proprietary food grade emulsifiers, preservatives, and other organics, and <1 % vitamin B12. The EVO solution was injected at 1 L/min simultaneously into the three injection wells over the course of 5.8 h.

2.3. Groundwater sampling

In 2009, groundwater was collected and filtered through an 8 μm pre-filter followed by a 0.2 μm sample filter, as described previously (Gihring et al., 2011). In 2017, groundwater was retrieved using a peristaltic pump, and prior to each sample, water levels were measured using an electric water level tape with a weighted probe (Solinst Canada Ltd., Georgetown, ON, Canada). Groundwater was collected 6 days prior to the injection on December 13, 2017, and 1, 8, 15, 22, 50, 78, 106, 134, and 372 days after the injection. Prior to groundwater collection, three well volumes were purged and an AquaTroll 9600 (In-situ, Fort Collins, CO, USA) was used to measure temperature, specific conductivity, dissolved oxygen, and pH. Groundwater was pumped at 250 mL/min and 10 L was collected in sterile amber glass bottles with no headspace then transported at 4 °C to be filtered. Successive filtrations were performed through a 10 μm polycarbonate (PCTE) filter followed by a 0.2 μm nylon or polyethersulfone (PES) filter using a peristaltic

pump (Sterlitech, Kent, WA, USA). Several samples required multiple filters due to clogging issues arising from the presence of oil. Filters were stored at −80 °C until DNA extraction was performed.

2.4. Geochemical and microbial abundance measurements

Geochemical measurements from 2009 were obtained from (Gihring et al., 2011). For the 2017 injection, an inductively coupled plasma mass spectrometer (ELAN 6100, PerkinElmer, Inc., Waltham, MA, USA) was used for trace elemental analysis. Ten mL of groundwater were collected in trace-clean tubes with 1 % nitric acid preservative for Na, Mg, Al, K, Ca, Sc, Fe, Mn, Tb, and U measurements, described previously (Lovley et al., 1996). Acetate, sulfate, and nitrate were analyzed using a Dionex ICP 5000+ (ThermoFisher, Waltham, MA, USA) with a stepwise KOH gradient on an AS-11 column with detection by electrical conductivity. Chromeleon software (ThermoFisher Scientific, Inc., Waltham, MA, USA) was used to perform calibrations and peak detection with manual peak integration. In 2009, microbial abundance was assessed using qPCR (Gihring et al., 2011). In 2017, the Acridine Orange Direct Count (AODC) method was used to assess cell numbers (Francisco et al., 1973). These measurements are not available for the time point of day 372.

2.5. DNA extraction and sequencing

In 2009 and 2017, DNA was extracted from 0.2 μm filters with a modified freeze-grind method. Briefly, PES filters were directly ground in liquid nitrogen, while nylon filters were partially submerged in liquid nitrogen and cut into roughly 2 x 2 mm pieces using sterile scissors before freeze-grinding. The resulting freeze-ground media was then incubated in a CTAB-based DNA extraction buffer with SDS, as described previously (Zhou et al., 1996). The crude DNA was precipitated by isopropanol and purified using DNeasy PowerSoil DNA isolation kits with the bead beating step omitted (Qiagen, Germantown, MD, USA). Amplicon libraries of the V4 region of the 16S rRNA gene were prepared using the modified two-step PCR approach as described (Wu et al., 2015) using 515F and 806R primers. Sequencing was performed using Illumina MiSeq with a 500-cycle v2 MiSeq reagent cartridge (Illumina, San Diego, CA, USA) as described (Caporaso et al., 2012). Amplification and sequencing for samples of the two injections were performed in 2014 (using material from 2009 stored at −80 °C re-sequenced on a MiSeq rather than with pyrosequencing) and 2018, respectively.

2.6. Sequence processing

The sequencing data were processed by USEARCH (version 11.0.667), including demultiplex, merge pairs with ≤10 mismatches and ≥ 80 % of alignment, trim primers without mismatch, and quality filtering with ≤1 expected error and ≥100 fragment length. FastQC was used to assess sequence quality (Andrews, 2024). Briefly, of the 4 sequencing runs performed, average Phred score was 37 in all cases. The raw sequence data are available at the NCBI SRA under accession ID PRJNA1084851. UNOISE3 was used to generate zOTU tables. For samples with multiple filters, a single sample was generated by resampling each zOTU table weighted by the amount of DNA obtained from each extraction. Taxonomy information was assigned by RDP Naïve Bayesian Classifier with the Silva 138 reference database (Callahan et al., 2016; Glöckner et al., 2017; Wang et al., 2007), using the function 'assignTaxonomy' in DADA2 (Callahan et al., 2016). Multiple sequence alignment was performed using MAFFT function in QIIME2 (version 2021.2) without masking (Bolyen et al., 2019; Katoh and Standley, 2013). FastTree (constrained; version 2.1.11) was used to construct phylogenetic trees (Price et al., 2009). Phylogenetic alpha and beta diversities were calculated using the IEG statistical analysis pipeline (http://ieg3.rccc.ou.edu:8080).

2.7. Statistical analyses

All statistical analyses were performed in R version 4.2 or 4.3, with randomly seeded functions using seed 0451. R function Ioncal (https://github.com/putt-ad/ioncal) was used to assess instrument performance and final calibrations. The package Phyloseq was used for data handling and diversity calculations (McMurdie and Holmes, 2013). The zOTU table was rarefied to 10,449 reads per sample using the rngseed 0451. R package vegan was used for Mantel tests between geochemical correlations (Oksanen et al., 2022). Function Maaslin2 from package Maaslin2 (Mallick et al., 2023) was used for differential abundance analysis of each injection separately using a cutoff of 1 % relative abundance in either 12.5 % (2009) or 10 % (2017) of samples in order to ensure the zOTU is present in sufficient wells at a single time point. Additionally, well identifier (i.e., location) was specified as a random effect and days after injection were used as the fixed effect, with the preinjection time point as reference. Otherwise, the default settings were used. Only zOTUs with a q-value of 0.05 or less and a coefficient greater than 1 (roughly a 2.7-fold change) during the reductive phase were selected for further analysis. Packages iCAMP and NST were used for iCAMP and NST analysis (Ning, 2022a, 2022b). For iCAMP, the default settings with no transformations were used. To ensure sufficient replicates for NST, samples were grouped according to the geochemical state of the injection (before, during, and after uranium reduction). For taxonomic NST, the null model "PF" was used, and for phylogenetic NST, phylogenetic shuffle was also incorporated. Otherwise, all NST calculations were run with the default settings. Code modified from the R package amplicon was used for alpha diversity visualization (Liu et al., 2023). Packages ggplot2, ggcorrplot, and ggheatmap were used for the visualization of results, in addition to the iTOL tool and itol.toolkit R package (Letunic and Bork, 2021; Zhou, 2023). Community-level 16S rRNA copy number analysis was performed as previously described (Dai et al., 2022). A full list of packages and code are available at https://github.com/jpmichael93/Publications.

3. Results

3.1. Geochemical variables

In 2009, uranium concentrations in the aquifer decreased from a mean of 1.9 mg L^{-1} to 0.3 mg L^{-1} by day 17 after EVO injection (Gihring et al., 2011). By the final time point of Day 269, uranium concentration was 1.05 mg L^{-1}. Uranium concentrations in the control wells ranged between 1.14 mg $L^{-1}$and 1.3 mg L^{-1} during the period. In 2017, uranium concentrations in the monitoring wells decreased from 2.0 mg L^{-1} to 0.5 mg L^{-1} after EVO injection (Fig. 1a), with the control well also dropping from 1.7 mg L^{-1} prior to the injection to 1.1–1.4 mg L^{-1} after the injection. Terminal electron acceptors such as nitrate, sulfate, and iron showed similar patterns to uranium (Table S1). In 2009, nitrate concentrations decreased from 13.3 mg L^{-1} to 1.2 mg L^{-1} by day 31. In 2017, nitrate decreased from 13.3 mg L^{-1} to 0.8 mg L^{-1} by Day 8. Sulfate had a lower minimum concentration in 2009 than in 2017 (6.3 mg L^{-1} in 2009 versus 23.0 mg L^{-1} in 2017). Iron remained at low levels throughout both injections, except on Day 8 in 2017, when it was elevated considerably in several wells. Acetate, a major products of EVO degradation, peaked at much greater concentrations in 2009 (maximum of 90.9 mg L^{-1} in 2009 versus 22.5 mg L^{-1} in 2017), but became undetectable by the end of the monitoring period in both 2009 and 2017 (Fig. 1b-e).

Measurements of specific conductivity, pH, Mn, Mg, Al, K, and Ca are shown in Table S1. Spearman's rank correlations of these geochemical species indicated that, in both years, acetate was negatively correlated with sulfate, uranium, and nitrate and positively correlated with manganese, iron, and magnesium ($|r|>0.4$, Fig. 1f). Sulfate, nitrate, and uranium were positively correlated with each other (Garcia, 2012). A Mantel test of the Spearman's rank correlations of these measurements

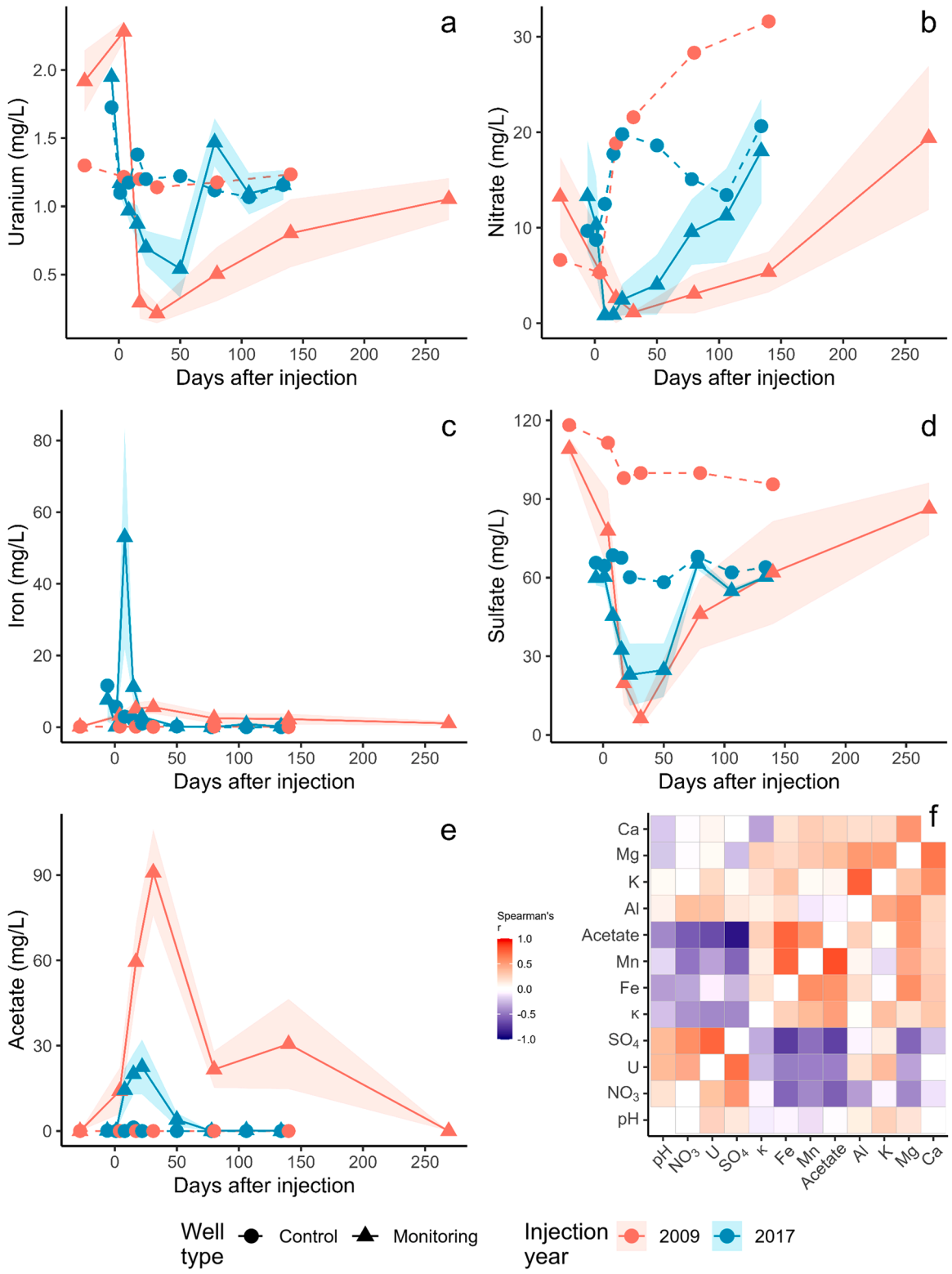

Fig. 1. Concentrations of selected geochemical species over the course of the injection and correlations between them. a) Uranium, mgL^{-1}. b) Nitrate, mgL^{-1}. c) Iron, mgL^{-1}. e) Sulfate, mgL^{-1}. f) Acetate, mgL^{-1}. f) Spearman's rank correlation coefficients between geochemical species in 2009 (upper triangle) and 2017 (lower triangle). a-e dashed lines and triangular points represent measurements from the control well. Shading represents +/- 1 standard error.

indicated that these correlations were strongly self-correlated (Mantel $r = 0.82$, $P = 0.001$, Fig. 1f), indicating that the directionality of the geochemical changes was consistent between 2009 and 2017.

3.2. Microbial abundance and α-diversities

U(VI) reduction and nitrate removal are mediated by indigenous microorganisms (Gihring et al., 2011; Zhou et al., 2014). Therefore, we examined microbial community succession after EVO injections.

Consistent with the stimulatory effect of EVO, abundances of microbes in groundwater measured by qPCR in 2009 or Acridine orange direct count in 2017, increased considerably following both injections (Fig. S1). In 2009, the measured abundance of microbes increased after the injection in all wells. In 2017, the abundance increased in all monitoring wells after Day 1. The control well FW215 showed comparable increases in 2009 but not in 2017, likely because of the larger quantity of EVO injected in 2009 refluxing into the control well.

Microbial α-diversities, calculated as Shannon index and Faith's phylogenetic diversity (PD), were decreased significantly ($p < 0.05$) after EVO injection in 2009 and returned to pre-injection levels at the end of the monitoring period (Fig. 2a, c; boxplots). Because of the overdosed EVO injection that caused reflux, the control well showed similar decreases in α-diversities, particularly in the time points immediately after the injection (Fig. 2a, c; red circles). For both taxonomic and phylogenetic indices in 2009, diversity remained significantly lower after the injection until the end of the monitoring period, though phylogenetic diversity decreased more than taxonomic diversity. In contrast, a significant decrease in microbial α-diversities was not detected until day 8 after the 2017 injection ($p < 0.05$, Fig. 2b, d). For both indices, diversity did not recover until Day 78 after the injection. As in 2009, phylogenetic alpha diversity decreased more than taxonomic alpha diversity. The α-diversities in the control well were relatively stable over the monitoring period in 2017 for both phylogenetic and taxonomic indices. Allen's phylogenetic entropy, the phylogenetic analog of Shannon α-diversity, was also significantly decreased after both EVO injections, including in the control well in 2009. It recovered to pre-injection levels by the end of each monitoring period (Fig. S2 c, d). Richness, the taxonomic analog of Faith's PD, showed similar trends to Allen's entropy (Fig. S2 a, b).

3.3. Microbial community compositions

Microbial communities in all wells, including the control, diverged from those of pre-injection during the 2009 injection. At the final time point of day 269, microbial communities returned to the pre-injection

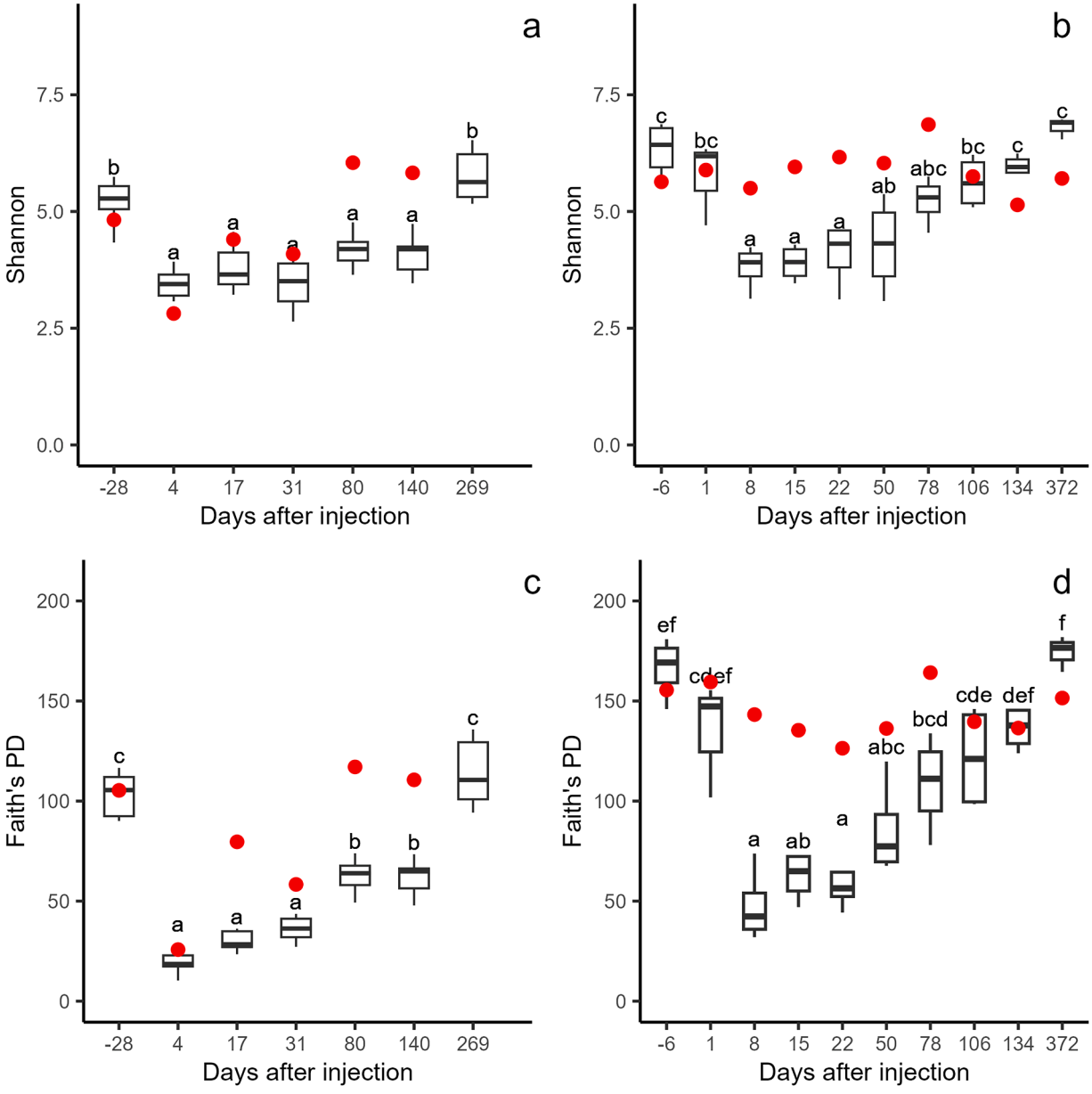

Fig. 2. Shannon diversity (a and b) and Faith's phylogenetic diversity (c and d) indices for 2009 (a and c) and 2017 (b and d). Red circles represent control well values. Different letters represent significantly different groups (ANOVA $p < 0.05$).

areas (Fig. 3a). Similarly, microbial communities had diverged by Day 8 after the EVO injection in 2017. The final time point of day 372 was the least dissimilar from pre-injection (Fig. 3b). Fitting of environmental variables showed that the maximal correlations between variables and communities were associated with similar time points. Uranium, nitrate, and sulfate decreased after both injections (Fig. 1a, b, d) and showed correlations with earlier time points in 2009 and later time points in 2017, with both surrounding pre-injection and control time points, while acetate and iron increased after injection (Fig. 1c, e) and correlated with the middle time points on both ordinations (Fig. 3a, b). Ordination within the same space revealed community shifts along the same axis over time but demonstrated that the 2017 injection promoted less dissimilarity than the 2009 injection (ANOSIM between control wells/pre-injection samples and monitoring wells divided by year; 2009 $r = 0.54$ $p = 0.01$, 2017 $r = 0.3$ $p = 0.01$) (Fig. 3c). Pairwise PERMANOVA analysis using a single grouping variable representing either control wells throughout each injection or specific time points was performed on a Bray-Curtis dissimilarity matrix representing all samples from both injections. Broadly, control communities and later time points from both injections showed less variance explained by the grouping variables compared to each other than during the time points closely following the injection, while those early time points were more similar to each other (Fig. 3d).

As the copy number of ribosomal RNA operons in bacterial genomes predicts microbial community growth rate and growth efficiency in response to nutrient availability (Roller et al., 2016; Wu et al., 2017), we calculated the community-averaged 16S ribosomal RNA copy number (*rrn*) for each sample. In 2009, *rrn* increased after the injection at Days 4 and 17 but decreased to pre-injection levels by Day 31. We observed the same trend in *rrn* after the injection in 2017, with an increase following the injection and a slow return to the pre-injection level as time progressed (Fig. S3).

We then evaluated zOTUs stimulated after the injection using Maaslin2. Approximately 8.5 % of zOTUs (602 out of 7032) were substantially (greater than 2.7-fold increase) and significantly stimulated during days 4, 17, 31, and 80 after injection in 2009 (Table S2), wherein uranium concentrations were decreased. We also identified 408 out of 9773 zOTUs, approximately 4.2 %, that were significantly stimulated

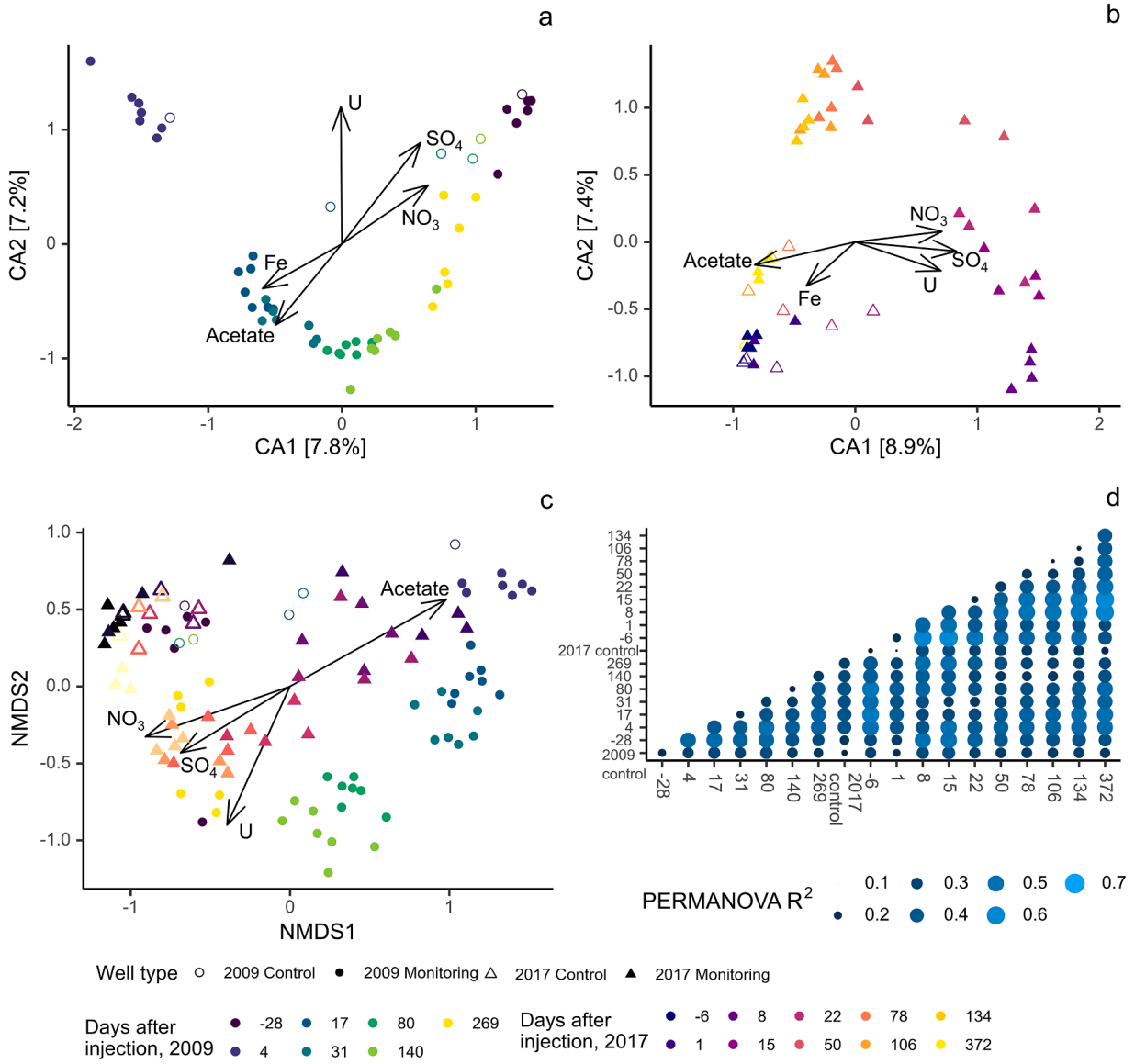

Fig. 3. CCA ordination of Bray-Curtis dissimilarity with fitted environmental variables of the 2009 injection (a) and 2017 injection (b). NMDS ordination of Bray-Curtis dissimilarity of both EVO injections within the same space (c). All environmental fits $p < 0.05$. Pairwise PERMANOVA R^2 values for each combination of timepoints.

after injection in 2017 on Days 8, 15, 22, and 50 (Table S2) when uranium concentrations were decreased. Notably, 242 zOTUs were stimulated by both 2009 and 2017 injections (Table S2). Among them, some zOTUs were affiliated with the genera *Pelosinus, Desulforegula, Geobacter,* and *Desulfovibrio*, identified as mediators of EVO degradation by (Gihring et al., 2011).

Numerous shared stimulated zOTUs have also previously been associated with uranium reduction. A total of 72 zOTUs identified as members of class Clostridia were identified as stimulated, generally appearing on days 17, 31, and 80 in 2009 and 15, 22, and 50 in 2017. Members of family Rhodocyclaceae (89 zOTUs) were also found to be frequently stimulated, and have previously been associated with uranium reduction (Martins et al., 2010). Most were stimulated at days 4, 17, and 31 in 2009 and 8, 15, and 22 in 2017, although some were also more prevalent in the latter portions of the injections (Table S2). Order Geobacterales was highly represented in the set of stimulated taxa (57), as were members of genera *Desulfovibrio* (15), *Desulfosporosinus* (17), and *Pseudomonas* (10), all of which have been shown to reduce uranium (Wall and Krumholz, 2006).

When classifying stimulated zOTUs into coarser phylogenetic levels (e.g., phylum or class), we found that 15 out of the top 20 classes were detected. However, there were notable differences between 2009 and 2017. Specifically, stimulation in 2017 was less intense but more broadly distributed among taxa. For example, *Desulforegula* was highly stimulated in 2009, reaching up to 60 % relative abundance in some wells (Fig. 4, Table S2). *Desulforegula* was also stimulated in 2017 but was only up to 15 % relative abundance in some wells (Fig. 4, Table S2). *Acidovorax* was present in 2009 prior to the injection at up to approximately 30 % relative abundance but was not stimulated by the injection, whereas in 2017 it became prevalent after the injection at up to 4 % relative abundance immediately after the injection, although numerous γ-Proteobacteria were stimulated and prevalent in both years (Fig. 4, Table S2). *Pelosinus* was stimulated in both years, but only reached a maximum of 15 % compared to 30 % in 2009. Notably, members of the NK4A214 group and others of order Oscillospirales followed similar trajectories in 2017 to those of *Pelosinus* in 2009, while also being stimulated in 2009 (Fig. 4, Table S2). Methanogens, primarily those from the class Methanomicrobia, were stimulated and became more prevalent in the later stages of the injection after uranium reduction ceased but were not notably stimulated in 2017 (Table S2).

3.4. Community assembly mechanisms

We evaluated the ecological processes underlying community dynamics after EVO injections. First, we used null model analysis to determine the normalized stochasticity ratio based on phylogenetic beta diversity (pNST). We observed identical trends in both injections: stochastic processes decreased after the EVO injections and then increased during the recovery phases (Fig. S4). In both years, pNST was approximately 75 % before the injection, at the final time points of both injections, and also in the control wells of both injections. Immediately following the injection, stochasticity decreased to approximately 25 %.

To further explore community assembly mechanisms, we used the iCAMP framework (Inferring Community Assembly Mechanisms by Phylogenetic bin-based null model analysis) (Ning et al., 2020). We observed an increase in selective processes after injection in both 2009

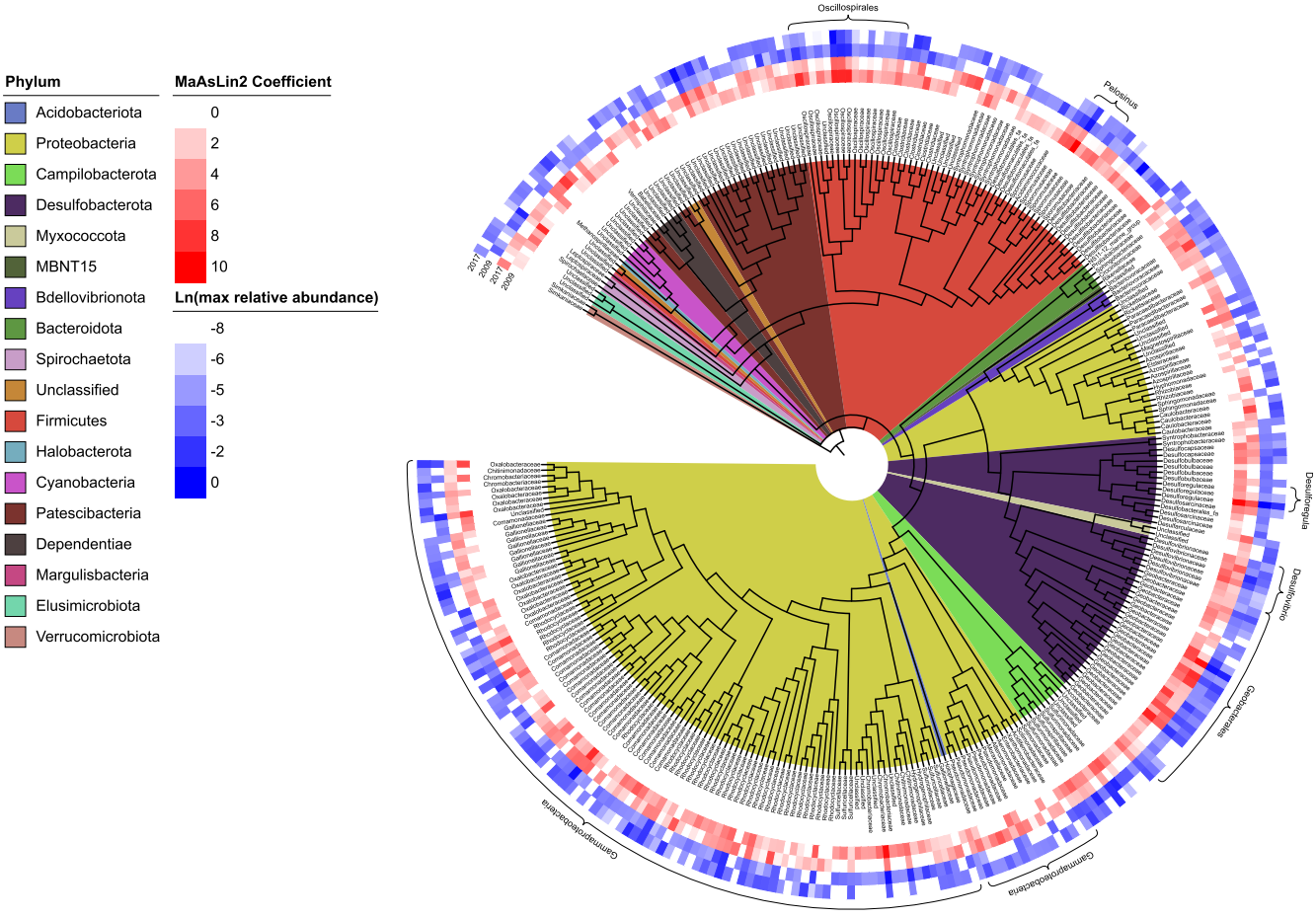

Fig. 4. Phylogenetic tree summary of stimulated taxa. Inner ring (red heatmaps) represents maximum MaAsLin2 coefficient (ln-fold change) achieved by the zOTU. Outer ring (blue heatmaps) represent the natural log of the max relative abundance achieved by the zOTU. Internal colors represent phyla, labels are families. Taxa discussed in the text are denoted by the outer brackets.

and 2017 (Fig. 5a, b). Before injection, stochastic processes, including dispersal limitation, homogenizing dispersal, drift, and others, showed a relative influence of approximately 60 % in 2009 and 80 % in 2017 but fell to lower than 30 % after the injection before returning to pre-injection levels by the final time point in both years. In both years, dispersal limitation was identified as the major stochastic process before and after the influence of EVO, as well as in the control wells throughout the injections. After the addition of EVO, dispersal limitation became a minor process, with drift and other stochastic processes (which varied much less than dispersal limitation) becoming more important to overall stochastic assembly when deterministic processes were most important. Deterministic processes, mainly homogeneous selection, had a stronger impact on stimulated taxa than non-stimulated taxa (Fig. 5c, d).

4. Discussion

We detected similar succession patterns in geochemistry, microbial community structure, and community assembly processes after EVO injections, with an 8-year interval between 2009 and 2017 and different amounts of injected EVO. In addition, we observed that comparable phyla, classes, and orders responded in similar ways between the two years, likely due to the influence of homogeneous selection observed after the injection. Fig. 6 shows a conceptual diagram of our results.

4.1. Reproducible patterns of geochemical responses to evo injections

EVO has been tested as a bioremediation agent because it is inexpensive and promotes longer-term reducing conditions than other aqueous injectates such as ethanol (Borden and Rodriguez, 2006). In 2017, we reduced the quantity of injectate from 3400 L to 1040 L because both data from the injection and operator observations implied that EVO injection quantity and speed countered the flow of groundwater. Regardless of EVO amount, we observed reducing conditions within the subsurface for at least 4 months following both injections (Table S1). However, uranium concentrations began rebounding after Day 31 and returned to pre-injection levels by the end of each monitoring period (Fig. 1a). Additionally, observed U minima were higher in 2017 than in 2009, likely due to the decreased EVO amount. This rebound was likely the result of not only influent U(VI) but also re-oxidation of biotically reduced U(IV), as well as decreases in other terminal electron acceptors critical to U reduction, most notably sulfate.

Alterations to groundwater geochemistry after both 2009 and 2017 injections proceeded in a thermodynamically favorable pattern, with decreases observed in nitrate, sulfate, uranium, and manganese and an increase in soluble (reduced) iron (Fig. 1, Table S1) and in agreement with our hypothesis i. Acetate peaked at much higher concentrations in 2009 than in 2017, which was likely caused by the higher amount of EVO injected in 2009 since acetate is produced during long-chain fatty acid oxidation (Fig. 1) (Sousa et al., 2009). However, the altered EVO quantity does restrict us from drawing major conclusions about the magnitude of geochemical change related to injection quantity – it is unclear whether we would have observed the long-term decrease in U concentrations with the same EVO amount, and the ways in which different quantities of EVO may alter the dispersal in the subsurface likely also impacted our results in indeterminate ways.

4.2. Reproducible patterns of microbial responses to EVO injections

At coarse phylogenetic resolution, the microbial community response to both EVO injections is very similar (Fig. 4), verifying hypothesis ii. Broadly, EVO injection stimulates Firmicutes, particularly the NK4A214 group of class Clostridia, first, followed by Desulfobacterota and then various nitrate, iron, or sulfate reducers, some of

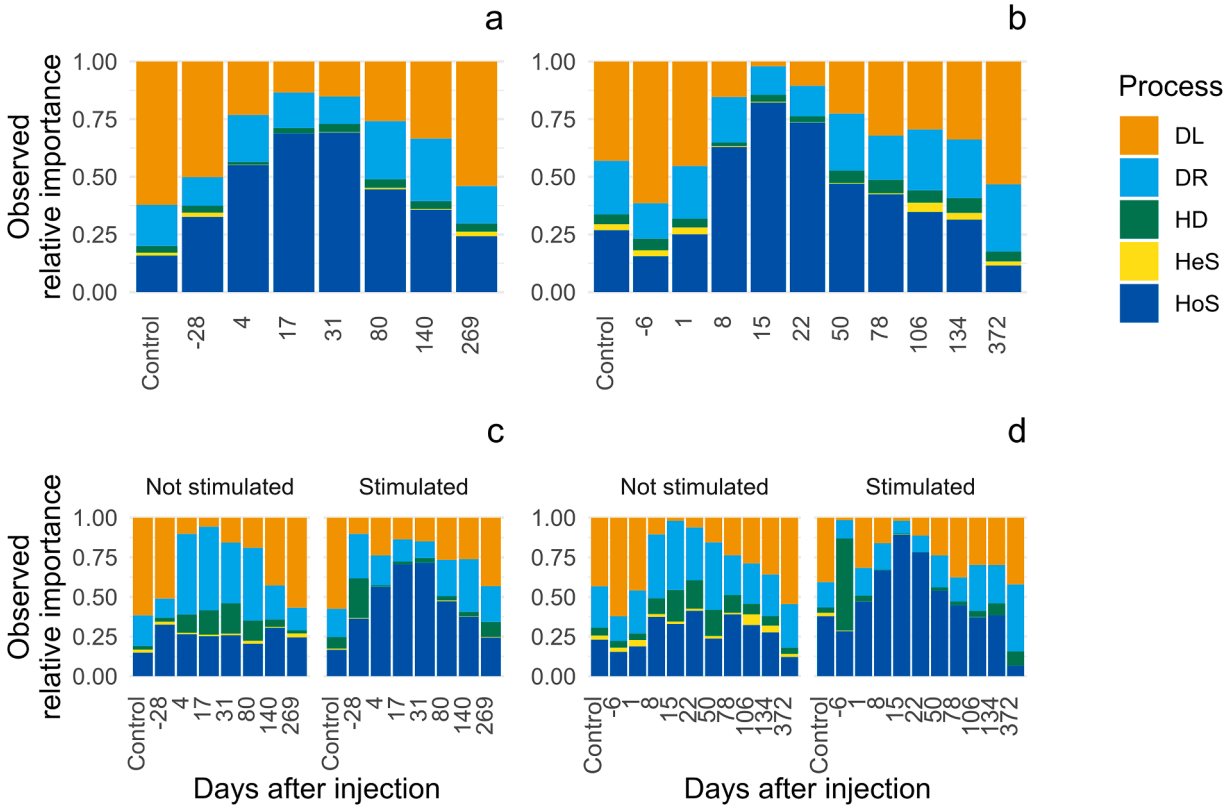

Fig. 5. Observed relative importance of dispersal limitation (DL), drift and other stochastic processes (DR.), homogenizing dispersal (HD), heterogeneous selection (HeS), and homogeneous selection (HoS) on microbial communities as a whole (a & b) or divided into categories based on stimulation status determined by MaAsLin2 (c & d). 2009 communities shown in a & c, 2017 in b & d.

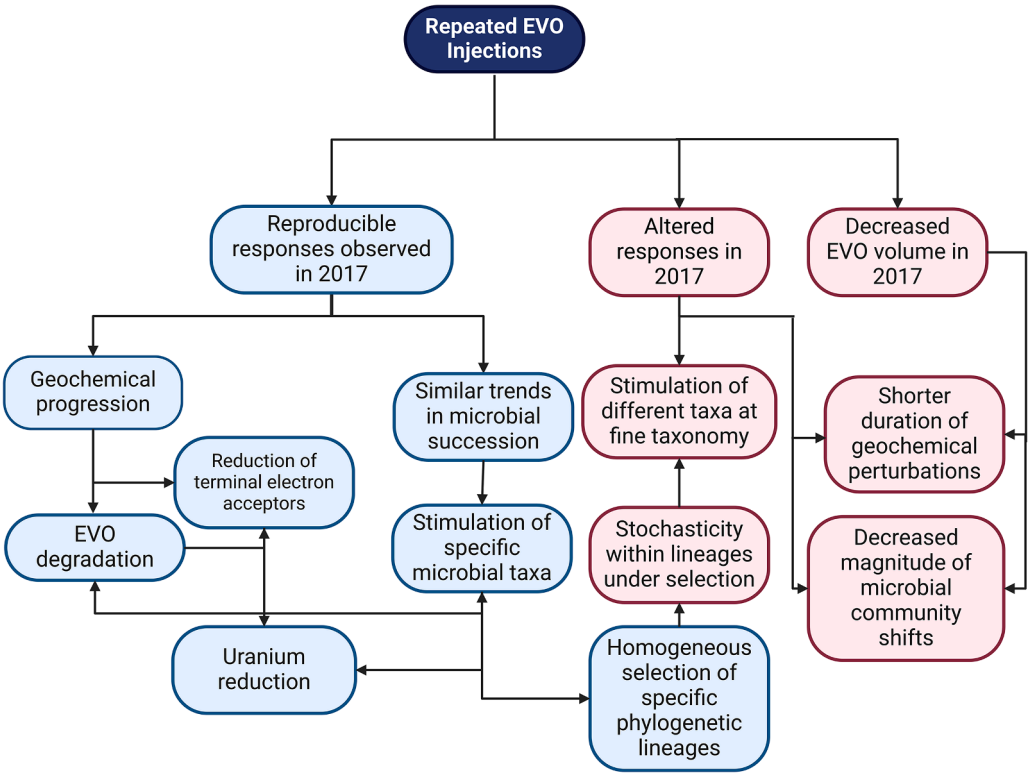

Fig. 6. Flowchart of the relationships between the injections and their respective outcomes. Repeated injections promote reproducible responses, which can be divided into geochemical and microbial successions. Geochemically, EVO degradation was coupled to the reduction of terminal electron acceptors including uranium. Microbially, we saw similar trends in microbial successions, primarily in the form of stimulation of specific taxa which degrade EVO, which was reflected in the homogeneous selection we observed, some of which ultimately reduce uranium. In terms of differences, the geochemical response in 2017 was more transient, and the communities did not diverge as much following the injection. Moreover, we observed stimulation of different taxa at the ASV level, likely driven by stochastic processes within those lineages. Created with BioRender.com.

which can also reduce uranium. Eventually, methanogens become prevalent. This broadens but still agrees with the conceptual model posited by Gihring et al., 2011 regarding the 2009 EVO injection. However, the fine patterns of microbial community stimulation differed between years. Of the 602 zOTUs stimulated in 2009 and 408 in 2017, only 235 were shared (39 % from 2009, 58 % from 2017). For example, a member of genus *Pelosinus*, a putative lipid hydrolyzer affiliated with the Firmicutes phylum (Gihring et al., 2011), was highly stimulated by the 2009 injection, peaking at over 30 % in some wells. In 2017, the response of the same zOTU of *Pelosinus* differs from 2009, peaking at 11 % (Fig. 4, Table S2). However, Firmicutes behaved similarly between 2009 and 2017, peaking around 35 % relative abundance at the early time points of the injection (Fig. 4, Table S2), possibly due to a rapid growth response to the new availability of nutrients (Wu et al., 2017). Similarly, the genus *Desulforegula*, belonging to the order Geobacterales was identified in 2009 as a likely mediator of long chain fatty acid (LCFA) oxidation (Gihring et al., 2011), but peaked at approximately 5 % relative abundance in 2017 compared to 20 % in 2009. However, Geobacterales responds consistently between the two years, peaking at roughly 25–30 % in both years, indicating that this activity could be conserved at this coarser taxonomic level (Fig. 4, Table S2). More broadly, both the stimulation and maximum relative abundances in 2017 were less than in 2009, demonstrating a weaker stimulation, which is expected given the substantial decrease in oil injected (Fig. 4). Without EVO injections, the Oak Ridge field site has a variety of abundant phyla including Proteobacteria, Nitrospirae, and Firmicutes, which were of high temporal variability (King et al., 2017). It is possible that the largely reproducible patterns of microbial responses to EVO injection arose from the 'microbial seed bank', which confers an advantage in response to environmental changes (Long et al., 2016). Thus, the seed bank of the Oak Ridge field site likely contained organisms capable of rapidly responding to EVO injection. To understand resiliency, information about rare organisms is critical to predicting community trajectories. For example, *Geobacter* was low in abundance at our study site (Table S2), yet acetate addition caused it to bloom and dominate the active microbial community (Anderson et al., 2003). *Geobacter, Desulfovibrio,* and members of the family Comamonadaceae consumed acetate while reducing nitrate, uranium, sulfate, and iron (Adav et al., 2010; Wall and Krumholz, 2006). The resulting carbon dioxide could be used by Methanobacteria and Methanomicrobia for methanogenesis, which has broader implications for the overall ecosystem function. Bicarbonate and acetate also stimulated the release of uranium adsorbed to ferric iron oxyhydroxide mineral surfaces, leading to a higher U (VI) reduction rate by *Geobacter* and other species (Long et al., 2015).

The dynamic succession of microbial community could be explained by the analogous r/K-strategy, which described the fast-growing r-strategists and slow-growing K-strategists (Wu et al., 2017). Nutrient addition shifts K-strategists toward r-strategists, as evidenced by increased community-averaged 16S *rrn* (Dai et al., 2022; Wu et al., 2017), which was also documented in this study (Fig. S3). At the end of the monitoring period, microbial communities returned to higher richness and biodiversity, showing a sign of K-strategy dominance (Fig. 2) (Cycoń et al., 2013).

4.3. Taxonomic resolution-dependent detection of community assembly processes

Determining the drivers of community structure and succession in response to environmental change is a central topic in ecology. Numerous previous studies demonstrated that both stochastic and

deterministic processes are important in controlling microbial community composition and structure, but their relative importance depends on individual ecosystems and environmental conditions (Zhou and Ning, 2017). In this study, we identified a transition to more deterministic community assembly following EVO amendment using the 16S rRNA gene and phylogenetic binning-based null model analysis. This is in direct contradiction to the pattern observed based on the functional gene composition and structure as detected by functional gene arrays and taxonomic null model analysis (and as such our hypothesis iii), which showed that the responses of microbial community functional gene structure to EVO injection were more stochastic (Zhou et al., 2014). We suspect that the apparent contradiction is most likely due to the differences in the taxonomic resolutions of the molecular markers used for analyzing community structure. Functional genes present on the arrays can have higher taxonomic resolution (e.g., strains, species) than the 16S rRNA gene-based approaches (e.g., genera, families) (Escalas et al., 2019; Louca et al., 2018; Martiny et al., 2015; Zhou et al., 2015). It seems that EVO injection selected for different phylogenetic lineages which are capable of rapidly using the injected EVO or its degradation products (e.g. within phylum Firmicutes during the initial oil degradation phase or within order Geobacterales during LCFA oxidation), which became overwhelmingly dominant compared to other community members. Thus, the measurable diversity of the microbial communities decreased, and the microbial community was largely deterministic based on 16S rRNA gene analysis. However, since more carbon substrates became available after EVO injection, more species/strains within the selected lineages could grow and coexist. Consequently, within those lineages stochastic birth and death would become very important and the diversity of the microbial communities based on functional genes increased after EVO injection (Zhou et al., 2014), all of which would result in the high importance of stochastic processes in shaping microbial community functional gene structure and succession following in EVO injection. However, with either of these markers we are unable to identify genomic features that could be responsible for the reproducibility we observed, including horizontal gene transfer of, for example, oil degradation genes, that may have been important to conferring redundant functionality to other members of subsurface communities. This could alter rates of EVO degradation or result in alternative lineages capable of degrading oil, leading to some of the differences in community structure that existed between the injections.

5. Conclusion

In this study, we compared the impacts of two EVO injections into the same groundwater wells separated by an 8-year gap at Oak Ridge, TN, USA, which was one of the largest nuclear waste disposal sites in the world. Despite a lower EVO dosage in 2017 compared to 2009, the injections promoted similar geochemical changes and microbial community successions governed by the shift from stochastic to deterministic community assembly based on 16S rRNA gene analysis. The microbial responses were conserved at a coarse phylogeny, but only approximately 50 % of responding zOTUs overlapped.

Our study empowers the merit of repeated longitudinal studies, which provide additional robust, reliable data than snapshots derived from single time points for testing theories about microbial community assembly and their responses to external perturbations. Future work can build upon the present results and investigate the rates of metabolite turnover and individual microorganisms more thoroughly. By addressing the challenge of validating the consistency and predictability of microbial responses, our study will be important for industrial applications of groundwater biostimulation by further constraining how the targeted microbial community will respond to nutrient injections.

Figure S1: The log (2) fold change in abundance from the pre-injection time point in 2009 measured by qPCR of 16S rRNA genes (a) and in 2017 measured by Acridine Orange direct count (b).

Figure S2: Richness and Allen's Entropy indices for 2009 (a and c) and 2017 (b and d). Red circles represent control measurements, different letters represent significantly different groups ($p < 0.05$).

Figure S3: Community average 16S rRNA gene copy number (rrn) in 2009 (a) and 2017 (b). Control points are represented by red dots.

Figure S4: Null model analysis for the 2009 injection (a) and the 2017 injection (b). Colors represent NST procedure; pNST used phyloshuffle (red), while tNST model PF (blue). Groups represent phases of the injection. Group 1 consists of day −28 in 2009 and days −6 and 1 in 2017. Group 2 consists of days 4, 17, 31, and 80 in 2009 and days 8, 15, 22, and 50 in 2017. Group 3 consists of days 140 and 269 in 2009 and days 78, 106, and 134 in 2017. The control group consists of all control well measurements.

Table S1: all geochemistries measured during the 2017 injections. The 2009 geochemistries were also shown in the supplemental material of Gihring et al., 2011.

Table S2: Stimulation coefficients and peak relative abundances for stimulated zOTUs. Coefficients are approximately ln-fold change. Blank entries indicate that the zOTU of interest was not stimulated in that year.

CRediT authorship contribution statement

Jonathan P. Michael: Writing – review & editing, Writing – original draft, Visualization, Investigation, Formal analysis, Data curation. **Andrew D. Putt:** Writing – review & editing, Writing – original draft, Methodology, Investigation, Formal analysis, Data curation. **Yunfeng Yang:** Writing – review & editing, Writing – original draft. **Benjamin G. Adams:** Writing – review & editing, Investigation, Data curation, Conceptualization. **Kathryn R. McBride:** Methodology, Investigation, Conceptualization. **Yupeng Fan:** Investigation, Data curation. **Kenneth A. Lowe:** Writing – review & editing, Resources, Investigation. **Daliang Ning:** Writing – review & editing, Writing – original draft, Supervision, Software, Resources, Project administration, Investigation, Formal analysis, Data curation. **Sindhu Jagadamma:** Writing – review & editing, Methodology, Investigation, Conceptualization. **Ji Won Moon:** Writing – review & editing, Methodology, Investigation, Conceptualization. **Dawn M. Klingeman:** Writing – review & editing, Methodology, Investigation, Conceptualization. **Ping Zhang:** Investigation, Data curation. **Ying Fu:** Resources. **Terry C. Hazen:** Writing – review & editing, Supervision, Project administration, Methodology, Funding acquisition, Conceptualization. **Jizhong Zhou:** Writing – review & editing, Supervision, Funding acquisition.

Declaration of competing interest

The authors declare that they have no known competing financial interests or personal relationships that could have appeared to influence the work reported in this paper.

Data availability

The data and code for this study has been uploaded to the SRA (sequences; accession PRJNA1084851) or Github.

Acknowledgments

This study by ENIGMA- Ecosystems and Networks Integrated with Genes and Molecular Assemblies (http://enigma.lbl.gov), a Science Focus Area Program at Lawrence Berkeley National Laboratory is based upon work supported by the U.S. Department of Energy, Office of Science, Office of Biological & Environmental Research under contract number DE-AC02-05CH11231. The community assembly mechanism tools used were developed under NSF Grants EF-2025558. The study was also supported by the Office of the Vice President for Research at the University of Oklahoma.

Supplementary materials

Supplementary material associated with this article can be found, in the online version, at doi:10.1016/j.watres.2024.121460.

References

Adav, S.S., Lee, D.J., Lai, J.Y., 2010. Microbial community of acetate utilizing denitrifiers in aerobic granules. Appl. Microbiol. Biotechnol. 85, 753–762. https://doi.org/10.1007/s00253-009-2263-6.

Anderson, R.T., Vrionis, H.A., Ortiz-Bernad, I., Resch, C.T., Long, P.E., Dayvault, R., Karp, K., Marutzky, S., Metzler, D.R., Peacock, A., White, D.C., Lowe, M., Lovley, D. R., 2003. Stimulating the In situ activity of geobacter species to remove uranium from the groundwater of a uranium-contaminated aquifer. Appl. Environ. Microbiol. 69, 5884–5891. https://doi.org/10.1128/AEM.69.10.5884-5891.2003.

Andrews, S., 2024. FastQC: A Quality Control Tool for High Throughput Sequence Data.

Bolyen, E., Rideout, J.R., Dillon, M.R., Bokulich, N.A., Abnet, C.C., Al-Ghalith, G.A., Alexander, H., Alm, E.J., Arumugam, M., Asnicar, F., Bai, Y., Bisanz, J.E., Bittinger, K., Brejnrod, A., Brislawn, C.J., Brown, C.T., Callahan, B.J., Caraballo-Rodríguez, A.M., Chase, J., Cope, E.K., Da Silva, R., Diener, C., Dorrestein, P.C., Douglas, G.M., Durall, D.M., Duvallet, C., Edwardson, C.F., Ernst, M., Estaki, M., Fouquier, J., Gauglitz, J.M., Gibbons, S.M., Gibson, D.L., Gonzalez, A., Gorlick, K., Guo, J., Hillmann, B., Holmes, S., Holste, H., Huttenhower, C., Huttley, G.A., Janssen, S., Jarmusch, A.K., Jiang, L., Kaehler, B.D., Kang, K.B., Keefe, C.R., Keim, P., Kelley, S.T., Knights, D., Koester, I., Kosciolek, T., Kreps, J., Langille, M.G.I., Lee, J., Ley, R., Liu, Y.X., Loftfield, E., Lozupone, C., Maher, M., Marotz, C., Martin, B.D., McDonald, D., McIver, L.J., Melnik, A.V., Metcalf, J.L., Morgan, S.C., Morton, J.T., Naimey, A.T., Navas-Molina, J.A., Nothias, L.F., Orchanian, S.B., Pearson, T., Peoples, S.L., Petras, D., Preuss, M.L., Pruesse, E., Rasmussen, L.B., Rivers, A., Robeson, M.S., Rosenthal, P., Segata, N., Shaffer, M., Shiffer, A., Sinha, R., Song, S.J., Spear, J.R., Swafford, A.D., Thompson, L.R., Torres, P.J., Trinh, P., Tripathi, A., Turnbaugh, P.J., Ul-Hasan, S., van der Hooft, J.J.J., Vargas, F., Vázquez-Baeza, Y., Vogtmann, E., von Hippel, M., Walters, W., Wan, Y., Wang, M., Warren, J., Weber, K. C., Williamson, C.H.D., Willis, A.D., Xu, Z.Z., Zaneveld, J.R., Zhang, Y., Zhu, Q., Knight, R., Caporaso, J.G., 2019. Reproducible, interactive, scalable and extensible microbiome data science using QIIME 2. Nat. Biotechnol. 37, 852–857. https://doi.org/10.1038/s41587-019-0209-9.

Borden, R.C., Rodriguez, B.X., 2006. Evaluation of slow release substrates for anaerobic bioremediation. Bioremediat. J. 10, 59–69. https://doi.org/10.1080/10889860600835492.

Callahan, B.J., McMurdie, P.J., Rosen, M.J., Han, A.W., Johnson, A.J.A., Holmes, S.P., 2016. DADA2: high-resolution sample inference from Illumina amplicon data. Nat. Methods 13, 581–583. https://doi.org/10.1038/nmeth.3869.

Caporaso, J.G., Lauber, C.L., Walters, W.A., Berg-Lyons, D., Huntley, J., Fierer, N., Owens, S.M., Betley, J., Fraser, L., Bauer, M., Gormley, N., Gilbert, J.A., Smith, G., Knight, R., 2012. Ultra-high-throughput microbial community analysis on the Illumina HiSeq and MiSeq platforms. ISME J. 6, 1621–1624. https://doi.org/10.1038/ismej.2012.8.

Chourey, K., Nissen, S., Vishnivetskaya, T., Shah, M., Pfiffner, S., Hettich, R.L., Löffler, F. E., 2013. Environmental proteomics reveals early microbial community responses to biostimulation at a uranium- and nitrate-contaminated site. Proteomics 13, 2921–2930. https://doi.org/10.1002/pmic.201300155.

Cycoń, M., Markowicz, A., Piotrowska-Seget, Z., 2013. Structural and functional diversity of bacterial community in soil treated with the herbicide napropamide estimated by the DGGE, CLPP and r/K-strategy approaches. Appl. Soil Ecol. 72, 242–250. https://doi.org/10.1016/j.apsoil.2013.07.015.

Dai, T., Wen, D., Bates, C.T., Wu, L., Guo, X., Liu, S., Su, Y., Lei, J., Zhou, J., Yang, Y., 2022. Nutrient supply controls the linkage between species abundance and ecological interactions in marine bacterial communities. Nat. Commun. 13, 175. https://doi.org/10.1038/s41467-021-27857-6.

Dangelmayr, M.A., Figueroa, L.A., Williams, K.H., Long, P.E., 2019. Characterizing organic carbon dynamics during biostimulation of a uranium contaminated field site. Biogeochemistry 143, 117–132. https://doi.org/10.1007/s10533-019-00553-w.

Deng, Y., Zhang, P., Qin, Y., Tu, Q., Yang, Y., He, Z., Schadt, C.W., Zhou, J., 2016. Network succession reveals the importance of competition in response to emulsified vegetable oil amendment for uranium bioremediation. Environ. Microbiol. 18, 205–218. https://doi.org/10.1111/1462-2920.12981.

Escalas, A., Hale, L., Voordeckers, J.W., Yang, Y., Firestone, M.K., Alvarez-Cohen, L., Zhou, J., 2019. Microbial functional diversity: from concepts to applications. Ecol. Evol. 9, 12000–12016. https://doi.org/10.1002/ece3.5670.

Fields, M.W., Bagwell, C.E., Carroll, S.L., Yan, T., Liu, X., Watson, D.B., Jardine, P.M., Criddle, C.S., Hazen, T.C., Zhou, J., 2006. Phylogenetic and functional biomakers as indicators of bacterial community responses to mixed-waste contamination. Environ. Sci. Technol. 40, 2601–2607. https://doi.org/10.1021/es051748q.

Francisco, D.E., Mah, R.A., Rabin, A.C., 1973. Acridine orange-epifluorescence technique for counting bacteria in natural waters. Trans. Am. Microsc. Soc. 92, 416–421. https://doi.org/10.2307/3225245.

Gandhi, T.P., Sampath, P.V., Maliyekkal, S.M., 2022. A critical review of uranium contamination in groundwater: treatment and sludge disposal. Sci. Total Environ. 825, 153947 https://doi.org/10.1016/j.scitotenv.2022.153947.

Garcia, C., 2012. A simple procedure for the comparison of covariance matrices. BMC. Evol. Biol. 12, 222. https://doi.org/10.1186/1471-2148-12-222.

Gihring, T.M., Zhang, G., Brandt, C.C., Brooks, S.C., Campbell, J.H., Carroll, S., Criddle, C.S., Green, S.J., Jardine, P., Kostka, J.E., Lowe, K., Mehlhorn, T.L., Overholt, W., Watson, D.B., Yang, Z., Wu, W.M., Schadt, C.W., 2011. A limited microbial consortium is responsible for extended bioreduction of uranium in a contaminated aquifer. Appl. Environ. Microbiol. 77, 5955–5965. https://doi.org/10.1128/AEM.00220-11.

Glöckner, F.O., Yilmaz, P., Quast, C., Gerken, J., Beccati, A., Ciuprina, A., Bruns, G., Yarza, P., Peplies, J., Westram, R., Ludwig, W., 2017. 25 years of serving the community with ribosomal RNA gene reference databases and tools. J. Biotechnol., Bioinfor. Solutions Big Data Anal. Life Sci. presented German Network Bioinf. Infrastruct. 261, 169–176. https://doi.org/10.1016/j.jbiotec.2017.06.1198.

Handley, K.M., Wrighton, K.C., Miller, C.S., Wilkins, M.J., Kantor, R.S., Thomas, B.C., Williams, K.H., Gilbert, J.A., Long, P.E., Banfield, J.F., 2015. Disturbed subsurface microbial communities follow equivalent trajectories despite different structural starting points. Environ. Microbiol. 17, 622–636. https://doi.org/10.1111/1462-2920.12467.

Katoh, K., Standley, D.M., 2013. MAFFT multiple sequence alignment software version 7: improvements in performance and usability. Mol. Biol. Evol. 30, 772–780. https://doi.org/10.1093/molbev/mst010.

King, A.J., Preheim, S.P., Bailey, K.L., Robeson, M.S.I., Roy Chowdhury, T., Crable, B.R., Hurt, R.A.Jr., Mehlhorn, T., Lowe, K.A., Phelps, T.J., Palumbo, A.V., Brandt, C.C., Brown, S.D., Podar, M., Zhang, P., Lancaster, W.A., Poole, F., Watson, D.B., W. Fields, M., Chandonia, J.M., Alm, E.J., Zhou, J., Adams, M.W.W., Hazen, T.C., Arkin, A.P., Elias, D.A., 2017. Temporal dynamics of in-field bioreactor populations reflect the groundwater system and respond predictably to perturbation. Environ. Sci. Technol. 51, 2879–2889. https://doi.org/10.1021/acs.est.6b04751.

Lakaniemi, A.M., Douglas, G.B., Kaksonen, A.H., 2019. Engineering and kinetic aspects of bacterial uranium reduction for the remediation of uranium contaminated environments. J. Hazard. Mater. 371, 198–212. https://doi.org/10.1016/j.jhazmat.2019.02.074.

Letunic, I., Bork, P., 2021. Interactive Tree Of Life (iTOL) v5: an online tool for phylogenetic tree display and annotation. Nucleic Acids Res. 49, W293–W296. https://doi.org/10.1093/nar/gkab301.

Li, B., Wu, W.M., Watson, D.B., Cardenas, E., Chao, Y., Phillips, D.H., Mehlhorn, T., Lowe, K., Kelly, S.D., Li, P., Tao, H., Tiedje, J.M., Criddle, C.S., Zhang, T., 2018. Bacterial community shift and coexisting/coexcluding patterns revealed by network analysis in a uranium-contaminated site after bioreduction followed by reoxidation. Appl. Environ. Microbiol. 84, e02885. https://doi.org/10.1128/AEM.02885-17. -17.

Li, L., Steefel, C.I., Kowalsky, M.B., Englert, A., Hubbard, S.S., 2010. Effects of physical and geochemical heterogeneities on mineral transformation and biomass accumulation during biostimulation experiments at Rifle, Colorado. J. Contaminant Hydrol., Front. Reactive Trans.: Microbial Dynamics nad Redox Zonation Subsurface 112, 45–63. https://doi.org/10.1016/j.jconhyd.2009.10.006.

Liu, Y.X., Chen, Lei, Ma, T., Li, X., Zheng, M., Zhou, X., Chen, Liang, Qian, X., Xi, J., Lu, H., Cao, H., Ma, X., Bian, B., Zhang, P., Wu, J., Gan, R.Y., Jia, B., Sun, L., Ju, Z., Gao, Y., Wen, T., Chen, T., 2023. EasyAmplicon: an easy-to-use, open-source, reproducible, and community-based pipeline for amplicon data analysis in microbiome research. Imeta 2, e83. https://doi.org/10.1002/imt2.83.

Long, P.E., Williams, K.H., Davis, J.A., Fox, P.M., Wilkins, M.J., Yabusaki, S.B., Fang, Y., Waichler, S.R., Berman, E.S.F., Gupta, M., Chandler, D.P., Murray, C., Peacock, A.D., Giloteaux, L., Handley, K.M., Lovley, D.R., Banfield, J.F., 2015. Bicarbonate impact on U(VI) bioreduction in a shallow alluvial aquifer. Geochim. Cosmochim. Acta 150, 106–124. https://doi.org/10.1016/j.gca.2014.11.013.

Long, P.E., Williams, K.H., Hubbard, S.S., Banfield, J.F., 2016. Microbial metagenomics reveals climate-relevant subsurface biogeochemical processes. Trends Microbiol. 24, 600–610. https://doi.org/10.1016/j.tim.2016.04.006.

Louca, S., Polz, M.F., Mazel, F., Albright, M.B.N., Huber, J.A., O'Connor, M.I., Ackermann, M., Hahn, A.S., Srivastava, D.S., Crowe, S.A., Doebeli, M., Parfrey, L.W., 2018. Function and functional redundancy in microbial systems. Nat. Ecol. Evol. 2, 936–943. https://doi.org/10.1038/s41559-018-0519-1.

Lovley, D.R., Coates, J.D., Blunt-Harris, E.L., Phillips, E.J.P., Woodward, J.C., 1996. Humic substances as electron acceptors for microbial respiration. Nature 382, 445–448. https://doi.org/10.1038/382445a0.

Lui, L.M., Majumder, E.L.-W., Smith, H.J., Carlson, H.K., von Netzer, F., Fields, M.W., Stahl, D.A., Zhou, J., Hazen, T.C., Baliga, N.S., Adams, P.D., Arkin, A.P., 2021. Mechanism Across scales: a holistic modeling framework integrating laboratory and field studies for microbial ecology. Front. Microbiol. 12 https://doi.org/10.3389/fmicb.2021.642422.

Mallick, H., Rahnavard, A., McIver, L., 2023. Maaslin2: "Multivariable Association Discovery in Population-scale Meta-Omics Studies. https://doi.org/10.18129/B9.bioc.Maaslin2.

Martins, M., Faleiro, M.L., da Costa, A.M.R., Chaves, S., Tenreiro, R., Matos, A.P., Costa, M.C., 2010. Mechanism of uranium (VI) removal by two anaerobic bacterial communities. J. Hazard. Mater. 184, 89–96. https://doi.org/10.1016/j.jhazmat.2010.08.009.

Martiny, J.B.H., Jones, S.E., Lennon, J.T., Martiny, A.C., 2015. Microbiomes in light of traits: a phylogenetic perspective. Science (1979) 350, aac9323. https://doi.org/10.1126/science.aac9323.

McMurdie, P.J., Holmes, S., 2013. phyloseq: an R package for reproducible interactive analysis and graphics of microbiome census data. PLoS. One 8, e61217. https://doi.org/10.1371/journal.pone.0061217.

Ning, D., 2022a. iCAMP: Infer Community Assembly Mechanisms By Phylogenetic-Bin-Based Null Model Analysis.

Ning, D., 2022b. NST: Normalized Stochasticity Ratio.

Ning, D., Yuan, M., Wu, L., Zhang, Y., Guo, X., Zhou, X., Yang, Y., Arkin, A.P., Firestone, M.K., Zhou, J., 2020. A quantitative framework reveals ecological drivers of grassland microbial community assembly in response to warming. Nat. Commun. 11, 4717. https://doi.org/10.1038/s41467-020-18560-z.

Oksanen, J., Simpson, G.L., Blanchet, F.G., Kindt, R., Legendre, P., Minchin, P.R., O'Hara, R.B., Solymos, P., Stevens, M.H.H., Szoecs, E., Wagner, H., Barbour, M., Bedward, M., Bolker, B., Borcard, D., Carvalho, G., Chirico, M., Caceres, M.D., Durand, S., Evangelista, H.B.A., FitzJohn, R., Friendly, M., Furneaux, B., Hannigan, G., Hill, M.O., Lahti, L., McGlinn, D., Ouellette, M.H., Cunha, E.R., Smith, T., Stier, A., Braak, C.J.F.T., Weedon, J., 2022. Vegan: community Ecology Package.

Ontiveros-Valencia, A., Zhou, C., Ilhan, Z.E., de Saint Cyr, L.C., Krajmalnik-Brown, R., Rittmann, B.E., 2017. Total electron acceptor loading and composition affect hexavalent uranium reduction and microbial community structure in a membrane biofilm reactor. Water Res. 125, 341–349. https://doi.org/10.1016/j.watres.2017.08.060.

Paradis, C.J., Miller, J.I., Moon, J.W., Spencer, S.J., Lui, L.M., Van Nostrand, J.D., Ning, D., Steen, A.D., McKay, L.D., Arkin, A.P., Zhou, J., Alm, E.J., Hazen, T.C., 2021. Sustained ability of a natural microbial community to remove nitrate from groundwater. Groundwater 60, 99–111. https://doi.org/10.1111/gwat.13132.

Price, M.N., Dehal, P.S., Arkin, A.P., 2009. FastTree: computing large minimum evolution trees with profiles instead of a distance matrix. Mol. Biol. Evol. 26, 1641–1650. https://doi.org/10.1093/molbev/msp077.

Roller, B.R.K., Stoddard, S.F., Schmidt, T.M., 2016. Exploiting rRNA operon copy number to investigate bacterial reproductive strategies. Nat. Microbiol. 1, 1–7. https://doi.org/10.1038/nmicrobiol.2016.160.

Smith, M.B., Rocha, A.M., Smillie, C.S., Olesen, S.W., Paradis, C., Wu, L., Campbell, J.H., Fortney, J.L., Mehlhorn, T.L., Lowe, K.A., Earles, J.E., Phillips, J., Techtmann, S.M., Joyner, D.C., Elias, D.A., Bailey, K.L., Hurt, R.A., Preheim, S.P., Sanders, M.C., Yang, J., Mueller, M.A., Brooks, S., Watson, D.B., Zhang, P., He, Z., Dubinsky, E.A., Adams, P.D., Arkin, A.P., Fields, M.W., Zhou, J., Alm, E.J., Hazen, T.C., 2015. Natural bacterial communities serve as quantitative geochemical biosensors. mBio 6, e00326. https://doi.org/10.1128/mBio.00326-15. -15.

Sousa, D.Z., Smidt, H., Alves, M.M., Stams, A.J.M., 2009. Ecophysiology of syntrophic communities that degrade saturated and unsaturated long-chain fatty acids. FEMS Microbiol. Ecol. 68, 257–272. https://doi.org/10.1111/j.1574-6941.2009.00680.x.

Tang, G., Watson, D.B., Wu, W.M., Schadt, C.W., Parker, J.C., Brooks, S.C., 2013. U(VI) Bioreduction with emulsified vegetable oil as the electron donor – model application to a field test. Environ. Sci. Technol. 47, 3218–3225. https://doi.org/10.1021/es304643h.

Thorgersen, M.P., Lancaster, W.A., Vaccaro, B.J., Poole, F.L., Rocha, A.M., Mehlhorn, T., Pettenato, A., Ray, J., Waters, R.J., Melnyk, R.A., Chakraborty, R., Hazen, T.C., Deutschbauer, A.M., Arkin, A.P., Adams, M.W.W., 2015. Molybdenum availability is key to nitrate removal in contaminated groundwater environments. Appl. Environ. Microbiol. 81, 4976–4983. https://doi.org/10.1128/AEM.00917-15.

Wall, J.D., Krumholz, L.R., 2006. Uranium reduction. Annu. Rev. Microbiol. 60, 149–166. https://doi.org/10.1146/annurev.micro.59.030804.121357.

Wang, Q., Garrity, G.M., Tiedje, J.M., Cole, J.R., 2007. Naive Bayesian classifier for rapid assignment of rRNA sequences into the new bacterial taxonomy. Appl. Environ. Microbiol. 73, 5261–5267. https://doi.org/10.1128/AEM.00062-07.

Wu, L., Wen, C., Qin, Y., Yin, H., Tu, Q., Van Nostrand, J.D., Yuan, T., Yuan, M., Deng, Y., Zhou, J., 2015. Phasing amplicon sequencing on Illumina Miseq for robust environmental microbial community analysis. BMC Microbiol. 15, 125. https://doi.org/10.1186/s12866-015-0450-4.

Wu, L., Yang, Y., Chen, S., Jason Shi, Z., Zhao, M., Zhu, Z., Yang, S., Qu, Y., Ma, Q., He, Z., Zhou, J., He, Q., 2017. Microbial functional trait of rRNA operon copy numbers increases with organic levels in anaerobic digesters. ISMe J. 11, 2874–2878. https://doi.org/10.1038/ismej.2017.135.

Zelaya, A.J., Parker, A.E., Bailey, K.L., Zhang, P., Van Nostrand, J., Ning, D., Elias, D.A., Zhou, J., Hazen, T.C., Arkin, A.P., Fields, M.W., 2019. High spatiotemporal variability of bacterial diversity over short time scales with unique hydrochemical associations within a shallow aquifer. Water Res. 164, 114917 https://doi.org/10.1016/j.watres.2019.114917.

Zhang, P., Wu, W.M., Van Nostrand, J.D., Deng, Y., He, Z., Gihring, T., Zhang, G., Schadt, C.W., Watson, D., Jardine, P., Criddle, C.S., Brooks, S., Marsh, T.L., Tiedje, J. M., Arkin, A.P., Zhou, J., 2015. Dynamic succession of groundwater functional microbial communities in response to emulsified vegetable oil amendment during sustained *in situ* U(VI) reduction. Appl. Environ. Microbiol. 81, 4164–4172. https://doi.org/10.1128/AEM.00043-15.

Zhou, J., Bruns, M.A., Tiedje, J.M., 1996. DNA recovery from soils of diverse composition. Appl. Environ. Microbiol. 62, 316–322. https://doi.org/10.1128/aem.62.2.316-322.1996.

Zhou, J., Deng, Y., Zhang, P., Xue, K., Liang, Y., Nostrand, J.D.V., Yang, Y., He, Z., Wu, L., Stahl, D.A., Hazen, T.C., Tiedje, J.M., Arkin, A.P., 2014. Stochasticity, succession, and environmental perturbations in a fluidic ecosystem. PNAS 111, E836–E845. https://doi.org/10.1073/pnas.1324044111.

Zhou, J., He, Z., Yang, Y., Deng, Y., Tringe, S.G., Alvarez-Cohen, L., 2015. High-throughput metagenomic technologies for complex microbial community analysis: open and closed formats. mBio 6. https://doi.org/10.1128/mbio.02288-14.

Zhou, J., Ning, D., 2017. Stochastic community assembly: does it matter in microbial ecology? Microbiol. Mol. Biol. Rev. 81, e00002–e00017. https://doi.org/10.1128/MMBR.00002-17.

Zhou, T., 2023. itol.toolkit: Helper Functions for "Interactive Tree Of Life.